*Sensors and Materials*, Vol. 8, No. 4 (1996) 239–249
MYU Tokyo

S & M 0243

# $NO_2$ Sensing by Means of $SnO_2$(Al) Thin Films Grown by the Rheotaxial Growth and Thermal Oxidation Technique

Guido Faglia, Gianpaolo Benussi, Laura Depero,
Giorgio Dinelli[1] and Giorgio Sberveglieri

Department of Chemistry and Physics of Materials
University of Brescia, Via Valotti 9, Brescia 25123, Italy
[1]ENEL Research Center, Brindisi, Italy

(Received October 31, 1994; accepted November 30, 1995)

***Key words***: gas sensor, thin film, tin compound

The preparation and the sensitivity to $NO_2$ of $SnO_2$(Al) thin films deposited by magnetron sputtering onto ceramic substrates are reported. The preparation technique consists of the successive deposition of two metal films at high temperature (300°C) followed by thermal oxidation at 520°C for 10 h, according to the rheotaxial growth and thermal oxidation (RGTO) method. A Pt meandering thin film was deposited on the back of the $Al_2O_3$ substrate as a heating element and temperature probe. The Al concentration in the alloy was varied from 0.5 at% to 5 at%. The material is polycrystalline with a preferential orientation in the (110) direction and with crystallite size equal to about 500 Å. $SnO_2$(Al) thin-film sensors show the greatest sensitivity ($\Delta R/R$ ) to $NO_2$ when the dopant concentration is equal to 3 at% and the working temperature is 300°C. The sensitivity towards 20 ppm of $NO_2$ in dry synthetic air reaches the value of 20 when the sensor is kept at 300°C. Under these conditions concentrations lower than 1 ppm were detected. The response to other interfering gases such as CO and $C_2H_5OH$ as a function of the working temperature was examined.

## 1. Introduction

The detection of nitrogen oxides ($NO_2$ and NO) produced from combustion processes and automobiles is very important since these gases are very harmful air pollutants—the short-term exposure limit (10 min) for $NO_2$ is equal to 5 ppm. Commercial devices, based on spectroscopic infrared analysis and chemiluminescence, are very bulky, large and difficult to use for *in situ* monitoring.

An important subject of research is the development of small low-cost sensors, able to detect $NO_2$ concentrations as low as 1 ppm. Many studies have been carried out on materials such as phthalocyanine mainly coupled with SAW devices, solid electrolytes, and semiconductor oxides such as $SnO_2$(In),[1,2] $SnO_2$-$Al_2O_3$,[2] $SnO_2$-$In_2O_3$[3] and $Al_2O_3$-$V_2O_5$[4] mixed oxides, $WO_3$[5] and ZnO.[6] Sensors based on semiconductor oxide are low in cost and show high stability even in corrosive environments. The transduced physical property is the resistance change caused by gas absorption over the sensor surface. The disadvantage due to interference from other gas and long time drift is that it prevents massive diffusion of oxides.

In this paper we present the sensing properties towards $NO_2$ of $SnO_2$(Al) thin films grown by the rheotaxial growth and thermal oxidation (RGTO) technique.[7] The Al concentration was varied in the range 0.5–5 at%.

## 2. Experimental

The RGTO technique consists of two processes. First thin metallic films were deposited by RF magnetron sputtering from a tin target on polished alumina substrates of $3 \times 3 \times 0.25$ mm$^3$, with a meandering Pt thin film on the back, acting either as a heating element or temperature sensor. During deposition the substrate was kept at 300°C, a temperature higher than the melting point of tin (rheotaxial growth). The thickness of the metallic film is equal to 300 nm.

After the tin deposition, while keeping the substrate at the same temperature without breaking the vacuum, Al from a metallic target was deposited by the same technique. Different samples with dopant concentrations ranging from 0.5 to 5 at% were grown.

Figure 1 shows a SEM micrograph of the surface. The metallic film consists of agglomerates, with dimensions ranging from 1 $\mu$m to 5 $\mu$m, which are not interconnected; hence the film is insulating.

The metal-semiconductor phase transformation (thermal oxidation) is achieved by keeping the thin film at 520°C in a synthetic air flow for 10 h. The thermal cycle together with current flow through the thin-film surface at constant bias is plotted in Fig. 2. Due to oxygen incorporation in the lattice, the volume increases about 30%, causing interconnection of the agglomerates and creating percolation paths for current flow.

Figure 3 shows the surface of the semiconductor film after thermal oxidation; the agglomerates are porous and the wrinkled surface is well suited for gas absorption.

To perform electrical measurement, the sensor is mounted on a TO-8 socket and introduced in the test chamber where the concentrations of $NO_2$ and interfering gases are varied in a constant air flow. For the well-oxidized thin film grown by the RGTO

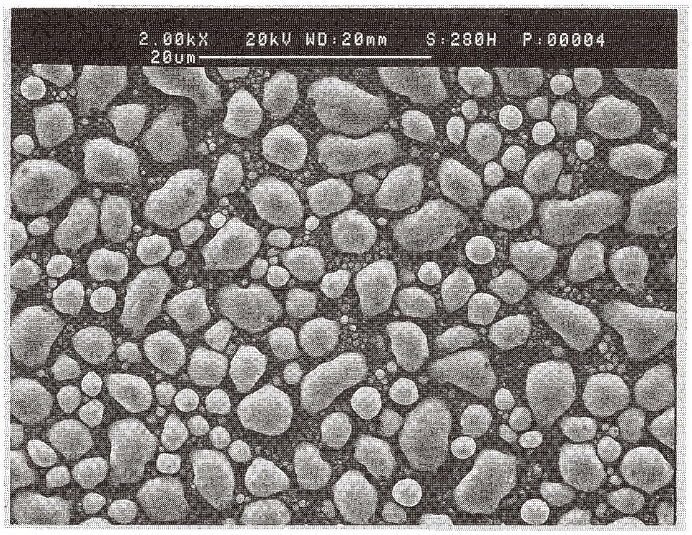


Fig. 1. SEM micrograph of the surface of a metallic alloy Sn-Al thin film after rheotaxial growth.

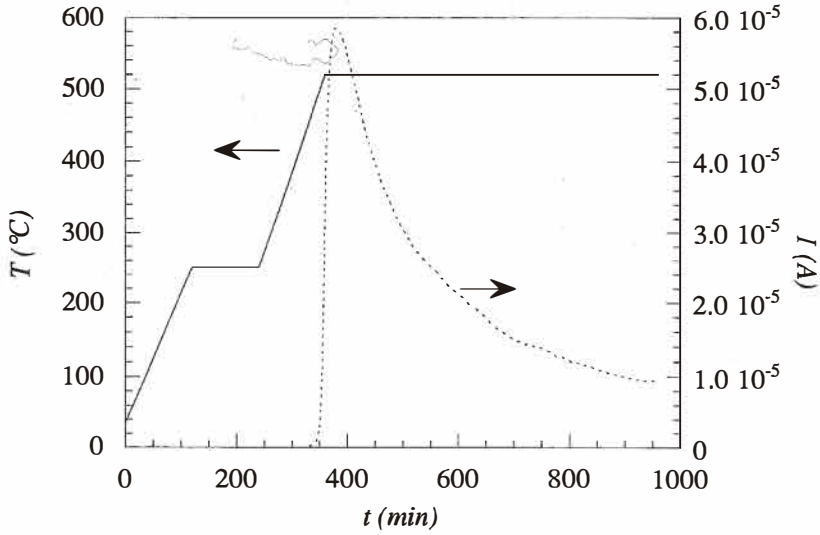


Fig. 2. Thermal cycle (solid line) performed to obtain the metal-semiconductor phase transformation, together with the current (dotted line) flowing through the surface in constant bias mode.

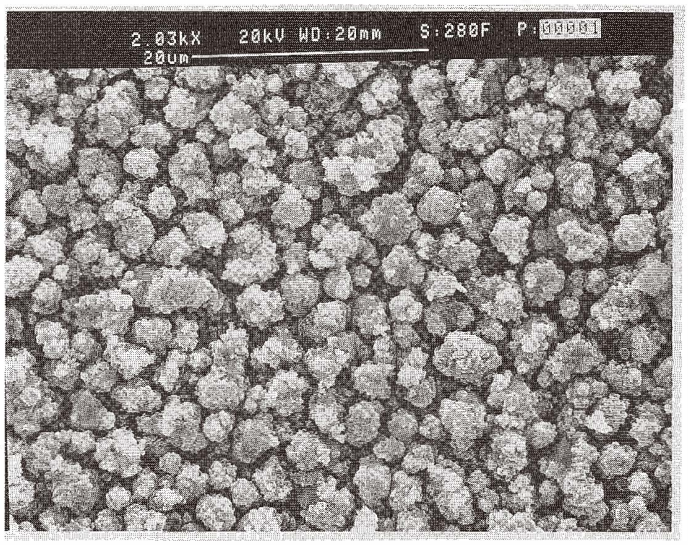


Fig. 3. SEM micrograph of a surface of $SnO_2$(Al) thin film after phase transformation (thermal oxidation).

technique, typical resistivity values obtained are $\rho = 10$ Ωcm. Moreover, Al introduction increases the resistivity since it behaves as an acceptor-type dopant inside the tin oxide lattice. Pt interdigitated contacts are grown by sputtering over the sensor surface to decrease the sensor resistance. The resistance is measured by a volt-amperometric technique at constant bias; recording of the current is carried out with a picoammeter. All the processes were controlled by a personal computer. The experimental setup is described elsewhere.[8]

## 3. Results and Discussion

X-ray diffraction (XRD) analysis performed on $SnO_2$(Al 0.5–5 at%) thin films grown on a glass substrate showed that the material is polycrystalline with a preferred orientation in the (110) direction with respect to the tin oxide powders. By applying the Scherrer equation to the (110) peak, the average grain size was estimated to be equal to about 50 nm. The results were independent of Al concentration.

As reported by Xu et al.,[9] trivalent ions such as $Al^{3+}$ act as dopant acceptors inside the tin oxide lattice, decreasing the carrier concentration and increasing the Debye length. By increasing the Al concentration at a constant average grain size, as in this case, the transducer function is governed by different mechanisms, such as grain boundary control when the grain mean radius $D$ is much greater than the Debye length $L_D$ neck control ($D \approx L_D$), and finally grain control ($L_D >> D$) where the sensitivity reaches its maximum value.

Figures 4(a) and 4(b) show the kinetic response (solid line) of a thin film during the introduction of 20 ppm of $NO_2$ (dotted line), when the sensor is kept at the operating temperatures of 250°C (a) and 350°C (b).

Tamaki *et al.*[10] studied nitrogen oxide absorption over tin oxide surfaces by TPD measurements and found that adsorbates originating from $NO_2$ are essentially the same as those from NO, since $NO_2$ molecules dissociate easily over tin oxide surfaces. These adsorbates can be divided into three different types: two nytrosil types, $Sn\text{-}NO^+$ and $Sn\text{-}NO^-$, and the nitrite type Sn-O-N = O. The nitrito type does not play a role in gas sensing since it is not involved in any electron exchange with the bulk of the semiconductor.

These results are in agreement with the work of Solymosi and Kiss [11] who proposed

$$NO_g + e^- \rightarrow NO^-_{chem}$$

$$NO_g \rightarrow NO^+_{chem} + e^-,$$

where the second type of adsorption is much weaker than the first one. Recently Ghiotti and coworkers [12,13] have proposed similar reactions based on FT-IR absorption measurements.

The shape of the kinetic response can then be explained by an increase in the height of surface barriers ($qV_s$) at grain interfaces due to electron trapping in NO chemisorbed molecules. The sample conductance decreases according to the law

$$G = G_0 e^{-\frac{qV_s}{kT}},$$

where $G_0$ is a term that contains the intragrain bulk conductance and $T$ the working temperature.

The initial peak, observed just after $NO_2$ introduction when the sensor working temperature is greater than 300°C, can be ascribed to $NO^+$ chemisorption, which is more favored at these temperatures but hindered after a few seconds by the most stable $NO^-$ form. These peak effects could be exploited for $NO_2$ identification.

The sensor response as a function of the Al concentration was investigated. The sensitivity towards 20 ppm of $NO_2$, defined as the relative change in sensor resistance with respect to synthetic air when steady-state conditions are reached, is shown in Fig. 5 as a function of the sensor working temperature. Different curves are obtained for different Al concentrations and the sensitivity for an undoped tin oxide sample is also reported. The temperature for maximum $NO_2$ sensitivity is equal to about 300°C. Under this operative conditions, there should be maximum coverage of the surface by $NO^-$ chemisorbed molecules. Figure 6 shows the sensitivity to 20 ppm of $NO_2$ at the working temperature of 300°C, relative to the Al concentration of the sample. Best performances are obtained with 3 at% doping; the sensitivity is equal to 20 and the improvement with respect to the undoped sample is about 5-fold.

The material responses to increasing concentrations of the oxidizing gas are shown for

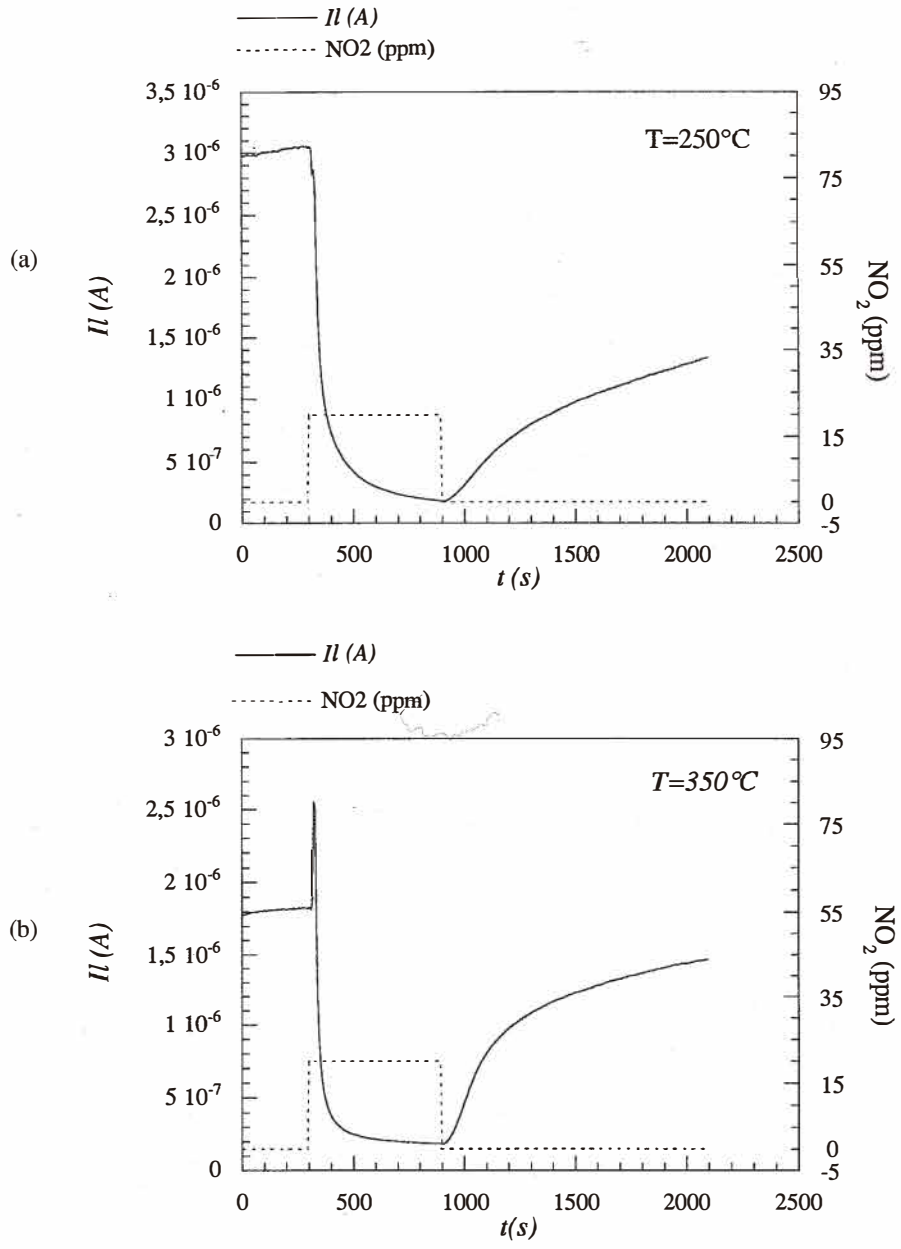


Fig. 4. Current flowing through the sensor and $NO_2$ concentration (dotted line) in synthetic air. The working temperatures are 250°C (a) and 350°C (b).

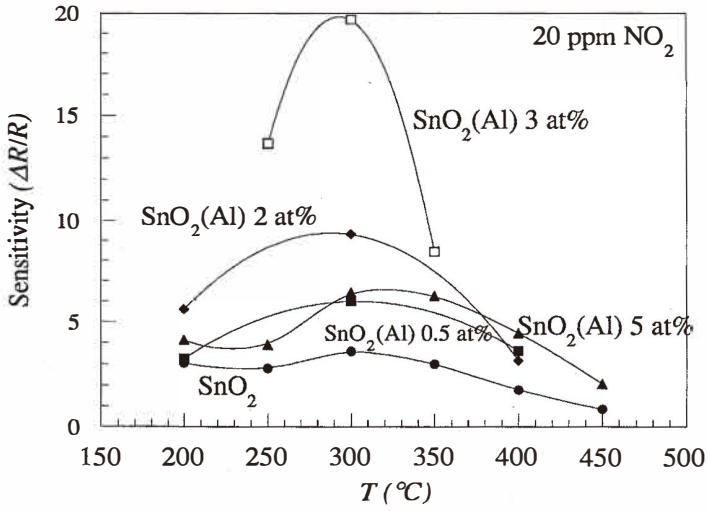


Fig. 5. Thin-film sensitivity ($\Delta R/R$) to 20 ppm of $NO_2$ versus the working temperature for an undoped tin oxide sample and for samples with different Al concentrations.

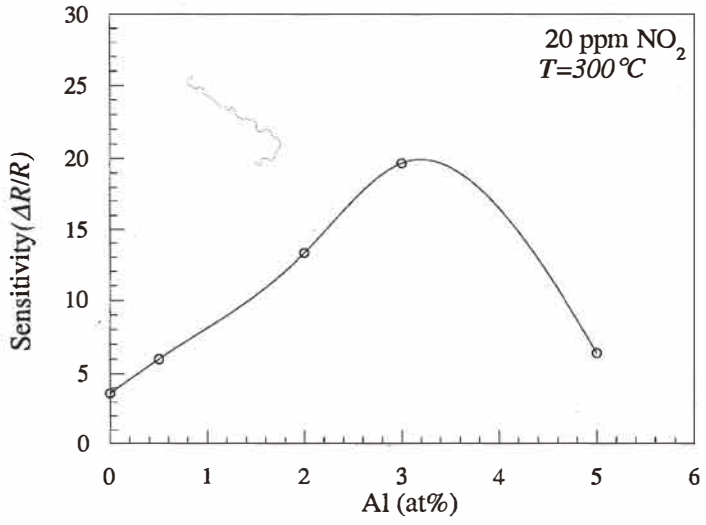


Fig. 6. Sensitivity to 20 ppm of $NO_2$ for samples kept at the working temperature $T_w$ = 300°C as a function of Al at%.

three working temperatures in Fig. 7. Sample doping is equal to 3 at%. Two main features can be considered: the first is that the material does not show any saturation effect up to nitrogen dioxide concentration equal to 20 ppm, so that it is possible to obtain the gas concentration from resistance measurements. The second aspect is that the sensor is able to detect $NO_2$ concentrations as low as 1 ppm, since the resistance doubles when the operating temperature is equal to 300°C.

Figure 8 shows the response time, defined as the time needed to reach 70% of the final current value after gas introduction, and Fig. 9 shows the recovery time, defined as the time needed to return to 70% of the initial current value after recovering to dry air flow, versus the working temperature. The recovery time decreases upon increasing the working temperature since thermodynamic equilibrium is reached more quickly. The same behavior should be reported for response times but the appearance of the current peak (see Fig. 4(b)) delays the attainment of steady-state conditions, making the curve flat.

Figure 10 shows the material response to interfering gases such as carbon monoxide and ethyl alcohol. These gases show a reduction behavior, reacting with ionosorbed oxygen ($O^-$ or $O_2^-$), and either diminishing the number of trapped electrons in surface states or decreasing the material resistance. Therefore the sensitivity is defined as the relative change in conductance with respect to dry air. Different working-temperature regions, where the material is sensitive to $NO_2$ (250–350°C) with respect to reducing gases (350–500°C), can be identified, so that selectivity can be achieved by changing the sensor temperature.

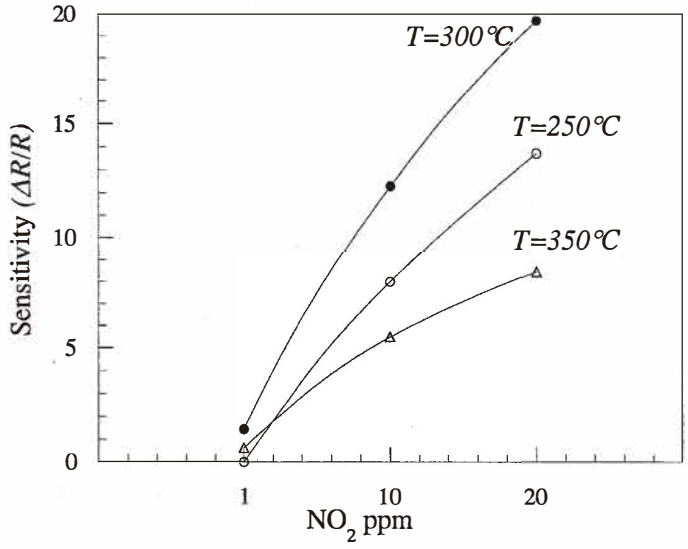


Fig. 7. Sensitivity as a function of $NO_2$ concentration for a $SnO_2$ (Al: 3 at%) sample. Results for three working temperatures are shown.

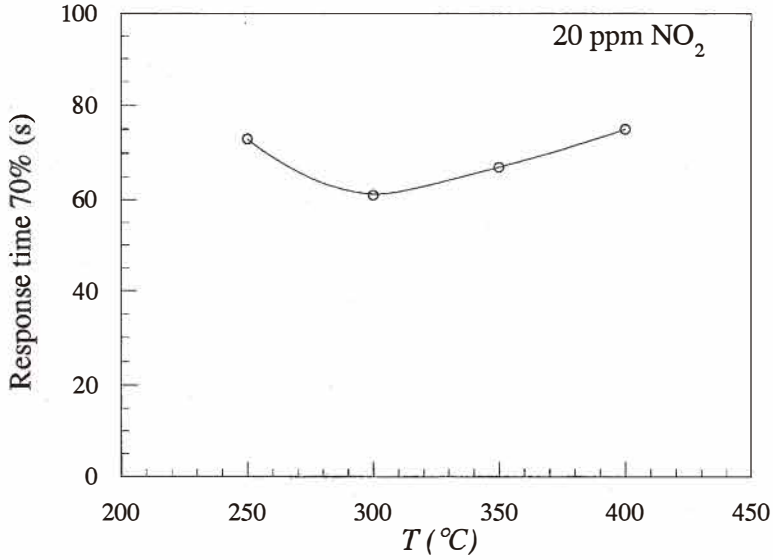


Fig. 8. Response time (70%) to 20 ppm of $NO_2$ as a function of the working temperature. The sample is $SnO_2$ (Al: 3 at%).

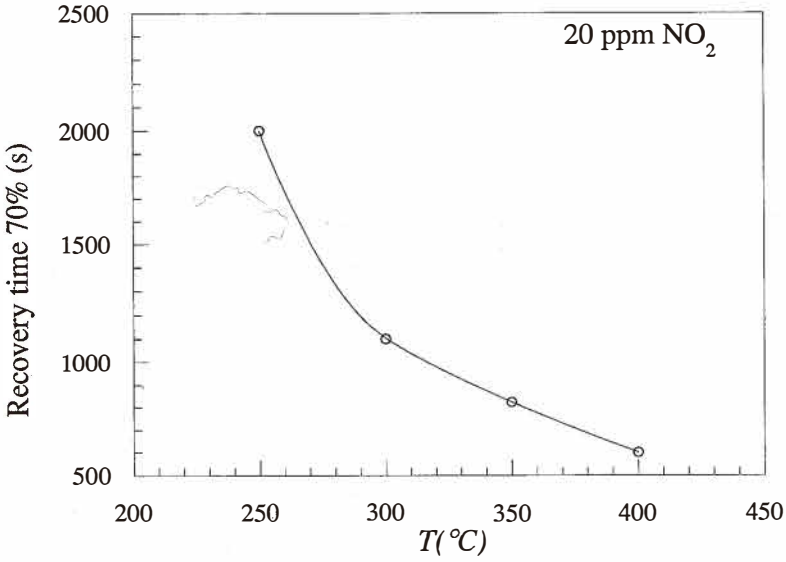


Fig. 9. Recovery time (70%) as a function of the working temperature after the introduction of 20 ppm of $NO_2$ followed by the introduction of dry air. The sample is $SnO_2$ (Al: 3 at%).

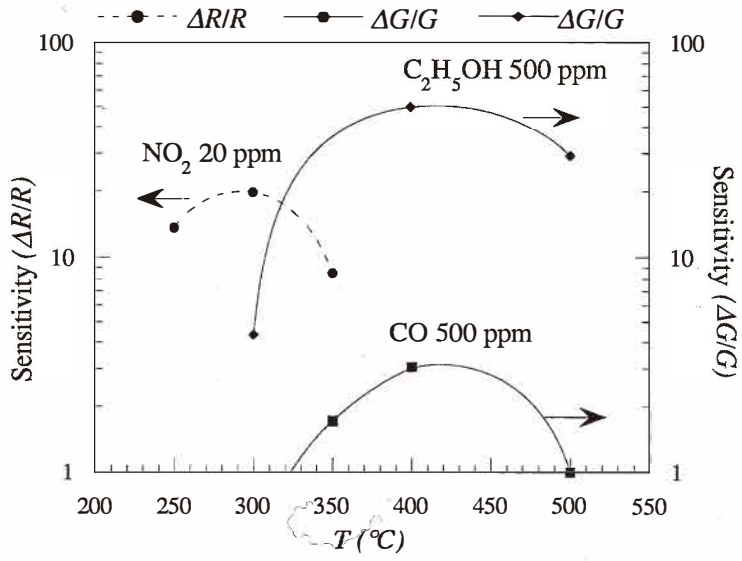


Fig. 10. Sensitivity to 20 ppm of $NO_2$ and interfering gases as a function of the operating temperature. The sensitivity is defined as $\Delta R/R$ for oxidizing gases and as $\Delta G/G$ for reducing ones.

## 4. Conclusions

$SnO_2$(Al) thin films are very promising sensors for $NO_2$ detection. Best performances were obtained when the dopant concentration was equal to 3 at% and the sensor was kept at 300°C. Under these operating conditions $NO_2$ concentration lower than 1 ppm was detected and selectivity towards reducing gases was achieved. Preliminary tests showed that the material is also stable after several $NO_2$ exposures, but some problems related to very long recovery time must be resolved. Periodic cleaning of the material surface by increasing the temperature might be a good method of overcoming these drawbacks.

## References

1 G. Sberveglieri, G. Faglia, S. Groppelli and P. Nelli: Sensors and Actuators **B8** (1992) 239.
2 G. Sberveglieri, S. Groppelli, P. Nelli, V. Lannto, H. Torvela, P. Romppainen and S. Leppavuori: Sensors and Actuators **B1** (1990) 79.
3 G. Sberveglieri, P. Benussi, G. Coccoli, S. Groppelli and P. Nelli: Thin Solid Films **186** (1990) 349.
4 T. Ishihara, K. Shiokawa, K. Eguchi and H. Arai: Sensors and Actuators **19** (1989) 256 .
5 N. Yamazoe and N. Miura: Gas Sensors: Principles, Operation and Developments (Kluwer Academic Publishers, Dortrecht, 1992) p. 1.
6 S. Matsushima, D. Ikeda, K. Kobayashi and G. Okada: Fourth International Meeting on Chemical Sensors, Tokyo (1992) p. 704.

7 G. Sberveglieri: Sensors and Actuators **B6** (1992) 239.
8 G. Sberveglieri, S. Groppelli, P. Nelli and A. Camanzi: Sensors and Actuators **B3** (1991) 189.
9 C. Xu, J. Tamaki, N. Miura and N. Yamazoe: Sensors and Actuators **B3** (1991) 147.
10 J. Tamaki, M. Nagaishi, Y. Teraoka, N. Miura and N. Yamazoe: Surface Science **221** (1989) 183.
11 F. Solymosi and J. Kiss: Journal of Catalysis **41** (1976) 202.
12 A. Chiorino, F. Boccuzzi and G. Ghiotti: Sensors and Actuators **B5** (1991) 189.
13 G. Ghiotti, A. Chiorino, W. X. Pan and L. Marchese: Sensors and Actuators **B7** (1992) 691.